Transcriptomic study of probenecid on injured spinal cords in mice

Yu-Xin Zhang Equal first author, [1], **Sai-Nan Wang** Equal first author, [1], **Jing Chen** [1], **Jian-Guo Hu** [1], **He-Zuo Lü** Corresp. [1]

[1] Clinical Laboratory, the First Affiliated Hospital of Bengbu Medical College, Bengbu, China

Corresponding Author: He-Zuo Lü
Email address: lhz233003@163.com

Background. Recent studies have found that probenecid has neuroprotective and repairing effects in the process of brain disorders. However, its effect on genome-wide transcription in acute spinal cord injury (SCI) is still unknown. Therefore, in this study, RNA sequencing (RNA-Seq) was used to analyze the effect of probenecid on the local expression of gene transcription 8 hours after injury. **Methods.** An Infinite Horizon impactor was used to perform contusive SCI in mice. The SCI model was made by using a rod (1.3 mm diameter) with a force of 50 kdynes. Sham-operated (sham) rats only received a laminectomy without contusive injury. The spinal cord injured mice were randomly assigned to the control or probenecid injection group. The drug (0.5mg/kg) was intraperitoneal injection immediately after injury. Eight hours after operation, the spinal cords were removed. The total RNAs were extracted and purified for library preparation and transcriptome sequencing. Differential gene expressions (DEGs) of three groups were analyzed by using the DESeq. Gene Ontology (GO) and Kyoto Encyclopedia of Genes and Genomes (KEGG) enrichment analysis of DEGs were performed by using GOseq R package and KOBAS. Real-time quantitative reverse-transcriptase polymerase chain reaction (RT-qPCR) was used to validate RNA-Seq results. **Results.** RNA-Seq showed that comparing with the solvent-control group, the number of DEGs was 641 in the probenecid-treated group (286 upregulated and 355 downregulated). According to GO analysis, DEGs were most enriched in extracellular matrix, collagen trimer, protein bounding and sequence specific DNA binding. KEGG analysis showed that the most enriched pathways included Cell adhesion molecules (CAMs), Leukocyte transendothelial migration, ECM-receptor interaction, PI3K-Akt signaling pathway, Hematopoietic cell lineage, Focal adhesion, Rap1 signaling pathway, etc. The sequence data have been deposited into Sequence Read Archive (https://www.ncbi.nlm.nih.gov/sra/PRJNA554464).

Transcriptomic study of probenecid on injured spinal cords in mice

Yu-Xin Zhang[1,2,3&], Sai-Nan Wang[1,2&], Jing Chen[1,2], Jian-Guo Hu[1,2*], He-Zuo Lü[1, 2*]

[1] Clinical Laboratory, the First Affiliated Hospital of Bengbu Medical College, Anhui 233004, P.R. China

[2]Anhui Key Laboratory of Tissue Transplantation, the First Affiliated Hospital of Bengbu Medical College, Anhui 233004, P.R. China

[3]Department of Biochemistry and Molecular Biology, Bengbu Medical College, Anhui 233030, P.R. China

& These authors contributed equally to this work

* Co-corresponding authors:

Jian-Guo Hu

Email address: jghu9200@163.com

He-Zuo Lü

Email address: lhz233003@163.com

Please address correspondence to:

He-Zuo Lü, M.D. Ph.D., Professor

Anhui Key Laboratory of Tissue Transplantation

the First Affiliated Hospital of Bengbu Medical College

287 Chang Huai Road

Bengbu 233004, P.R. China

Tel: +86-552-3170692

E-mail: lhz233003@163.com

Abstract

Background. Recent studies have found that probenecid has neuroprotective and repairing effects in the process of brain disorders. However, its effect on genome-wide transcription in acute spinal cord injury (SCI) is still unknown. Therefore, in this study, RNA sequencing (RNA-Seq) was used to analyze the effect of probenecid on the local expression of gene transcription 8 hours after injury.

Methods. An Infinite Horizon impactor was used to perform contusive SCI in mice. The SCI model was made by using a rod (1.3 mm diameter) with a force of 50 kdynes. Sham-operated (sham) rats only received a laminectomy without contusive injury. The spinal cord injured mice were randomly assigned to the control or probenecid injection group. The drug (0.5mg/kg) was intraperitoneal injection immediately after injury. Eight hours after operation, the spinal cords were removed. The total RNAs were extracted and purified for library preparation and transcriptome sequencing. Differential gene expressions (DEGs) of three groups were analyzed by using the DESeq. Gene Ontology (GO) and Kyoto Encyclopedia of Genes and Genomes (KEGG) enrichment analysis of DEGs were performed by using GOseq R package and KOBAS. Real-time quantitative reverse-transcriptase polymerase chain reaction (RT-qPCR) was used to validate RNA-Seq results.

Results. RNA-Seq showed that comparing with the solvent-control group, the number of DEGs was 641 in the probenecid-treated group (286 upregulated and 355 downregulated). According to GO analysis, DEGs were most enriched in extracellular matrix, collagen trimer, protein bounding and sequence specific DNA binding. KEGG analysis showed that the most enriched pathways included Cell adhesion molecules (CAMs), Leukocyte transendothelial migration, ECM-receptor interaction, PI3K-Akt signaling pathway, Hematopoietic cell lineage, Focal adhesion, Rap1 signaling pathway, etc. The sequence data have been deposited into Sequence Read Archive (https://www.ncbi.nlm.nih.gov/sra/PRJNA554464).

Introduction

Spinal cord injury (SCI) is defined as a variety of injuries to the spinal cord. According to the severity of injury may cause a variety of symptoms, ranging from pain to complete loss of movement and sensory function. SCI affects millions of people worldwide and usually affects patients for life (Friedli et al. 2015). In the United States, the incidence of SCI ranges from 12,000 to 20,000 cases a year, with more than 280,000 patients sitting in wheelchairs (Singh et al. 2014). In the past decade, the SCI cases in China have increased tenfold, and now 60,000 cases are added every year (Qiu 2009). SCI has a high rate of disability and mortality, which brings heavy burden to patients, families and society (Krueger et al. 2013). Therefore, it is self-evident to explore the effective treatment methods for repairing SCI in order to improve the quality of life of patients and reduce the burden of social medical care.

According to the different stages, the pathological processes following traumatic SCI can be divided into primary injury and secondary injury (Geisler et al. 2002; McDonald & Sadowsky 2002). Primary injury refers to the direct injury of the spinal cord by mechanical force, including compression, contusion, laceration and penetration. Secondary injury refers to edema, ischemia, local inflammation and electrolyte changes. These changes can cause accumulation of lipid peroxides and oxygen free radicals, release of inflammatory factors and proteases, and lead to a large number of cell apoptosis or necrosis, which further aggravates the damage of neurons and axons (Ahuja et al. 2017; Oyinbo 2011; Tran et al. 2018).

Probenecid is an organic anion transport protein inhibitor, which has been widely used in clinic (Hagos et al. 2017; Tollner et al. 2015). For example, probenecid has been used as a synergist in the treatment of gout and antibiotics. Its pharmacokinetics and side effects have been deeply studied (Baranova et al. 2004; Papadopoulos & Verkman 2008). Recent studies have found that probenecid can reduce the degree of cognitive impairment in rats with cognitive impairment (Mawhinney et al. 2011). Probenecid can also reverse cerebral ischemic injury and cellular inflammation (Wei et al. 2015; Xiong et al. 2014). These reports indicate that probenecid has neuroprotective and repairing effects in the process of central nervous system (CNS) injury. However, whether the drug can play a role in SCI and whether it can affect the gene expression profiles in injured spinal cords are still not reported in detail.

In this study, probenecid was injected intraperitoneally into spinal cord injured mice immediately after injury. Eight hours after operation, the spinal cords were removed, and RNA-Seq was used to analyze the changes of transcriptome expression in the injured area, then the key molecules and signal pathways were screened and identified, and provided new theoretical and experimental basis for SCI clinical treatment.

Materials & Methods

Animals

A total of 27 healthy and clean C57BL/6 female mice (18-20g, 8 weeks old) were used to model SCI. The animal care and use committee of Bengbu Medical College provided full approval for this research (037/2017).

Contusive SCI and drug injection

An Infinite Horizon impactor (Precision Systems & Instrumentation, Lexington, KY) was used to perform contusive SCI. The mice were firstly anesthetized with 50 mg/kg pentobarbital, then the T9 lamina was excised, the SCI model was made by using a rod (1.3 mm diameter) with a force of 50 kdynes. Sham-operated (sham) mice only received a laminectomy without contusive injury.

The spinal cord injured mice were randomly assigned to the solvent control or probenecid injection group. The solvent or probenecid (250mg/kg) was intraperitoneal injection immediately after injury. The solution (pH 7.3) was prepared according to Hainz's method (Hainz et al. 2017).

RNA isolation, quantification and qualification

Eight hours after operation, the mice were anesthetized and perfused with 10 ml PBS, and then the spinal cords (0.5 cm including the injury center) were removed. The total RNAs from spinal cords were extracted and purified using our previous methods (Shi et al. 2017).

Library preparation and transcriptome sequencing

The sequencing libraries were produced by using NEBNext® Ultra™ RNA Library Prep Kit for Illumina® (NEB, USA) according to our previous methods (Shi et al. 2017). Finally, the 125 bp/150 bp paired-end reads were we obtained and sequenced on an Illumina Hiseq platform.

Analysis of differential gene expression

Before analysis of differential gene expression, the gene expression statistics were analyzed by using RSEM software (http://deweylab.biostat.wisc.edu/rsem/) to convert the read count numbers to Fragments Per Kilobase of transcript per Million fragments mapped (FPKM), and Principal Component Analysis (PCA) analysis was made to determine the similarity and difference of data. Differential gene expression of three groups was analyzed according to our previous methods (Shi et al. 2017) by using the DESeq software (http://www.bioconductor.org/). Benjamini and Hochberg's approach was used to control the false discovery rate and adjust the

P-values. The adjusted P-value < 0.05 was defined as a standard for significant differences in gene expression.

Gene Ontology (GO) and Kyoto Encyclopedia of Genes and Genomes (KEGG) enrichment analysis of DEGs

The GO and KEGG analysis were performed by using GOseq R package and KOBAS software according to our previous methods (Shi et al. 2017).

Real-time quantitative reverse-transcriptase polymerase chain reaction (RT-qPCR)

To validate RNA-Seq results, 9 DEGs were randomly selected and verified by RT-qPCR according to our previous methods (Shi et al. 2017). PCR primer sequences are listed in Table 1. The relative quantitative results of each group of genes were calculated according to the formula of $^{\Delta\Delta}$Ct (Livak & Schmittgen 2001).

Results

Identification of expressed transcripts the mice spinal cords

For the quality assessment of sequencing data, 9 cDNA libraries were established, including sham (sham_1, sham_2 and sham_3), SCI (solvent control) (SCI_C1, SCI_C2 and SCI_C3) and SCI (probenecid) (SCI_P1, SCI_P2 and SCI_P3). RNA-Seq produced 48848744 to 61037096 raw reads for each sample. After filtering out the low-quality reads, the clean reads were from 48226002 to 60037772, with the Q30 (%) from 93.67 to 94.31 (Table 2).

In order to elaborate the source of variation in the original data, PCA analysis was conducted. As shown in Fig.1, PC1, PC2 and PC3 were 54.51%, 12.33% and 7.09%, respectively. This demonstrated that the data could be used for the next analysis.

The effect of probenecid on gene expression

RPKM and DEGSeq were used to analyze the gene expression level and the differential expression profiles, respectively. The results showed that comparing with the sham group, there were 4617 DEGs in SCI (solvent control) group, including 2904 up-regulated and 1713 down-regulated genes (Fig.2A and Table S1). Compared with the SCI (solvent control), there were 641 different genes in SCI (probenecid) group, 286 were up-regulated and 355 were down-regulated (Fig.2B and Table S1). The sequence data have been deposited into Sequence Read Archive (https://www.ncbi.nlm.nih.gov/sra/PRJNA554464). BioSample accessions are SAMN12268369, SAMN12268370, SAMN12268371, SAMN12268372, SAMN12268373, SAMN12268374, SAMN12268363, SAMN12268364 and SAMN12268365.

RT-qPCR identification of DEGs

In order to verify the RNA-Seq results, 9 DEGs were randomly selected from SCI (probenecid) compared with SCI (solvent control) group, namely Itga1, Lamb1, Cldn5, Lama2, CD34, Esam, Setdb2, Agrn and Ccnt2. The results indicated that these DEGs' expression patterns were similar between RNA-Seq and RT-qPCR (Fig.3).

Cluster Analysis of DEGs

The DEGs in different groups were analyzed by using FPKM hierarchical cluster analysis. As shown in Fig. 4, DEGs were classified into different expression cluster by hierarchical clustering. These clusters contained up-regulated or down-regulated DEGs. Most of the DEGs up-regulated in SCI (solvent control) group compared to sham group were in the middle and upper clusters, while down-regulated genes were observed in the lower cluster. Comparing to sham group, most of the DEGs up-regulated in SCI (probenecid) group were in the upper cluster, while down-regulated genes were mainly observed in the lower cluster. Comparing with SCI (solvent control) group, some up-regulated DEGs in SCI (probenecid) group were found in upper cluster, while

down-regulated DEGs were observed in the middle cluster, there are also some clusters with no significant differences.

Go enrichment analysis of DEGs

Comparing with sham group, 78 GO terms in up-regulated DEGs (Fig.5A, Table S2) and 9 GO terms in down-regulated DEGs (Fig.5B, Table S2) were found in SCI (solvent control) group. The up-regulated DEGs were most enriched in binding, protein binding, chemokine activity, chemokine receptor binding, G-protein coupled receptor binding, anion binding, small GTPase mediated signal transduction, immune system process, immune response, etc. The down-regulated DEGs were most enriched in protein binding, binding, extracellular-glutamate-gated ion channel activity, acid phosphatase activity, transporter activity, mannose metabolic process, excitatory extracellular ligand-gated ion channel activity, transmembrane transporter activity, anion transmembrane and transporter activity. In SCI (probenecid) group, 3 GO terms in down-regulated DEGs (Fig.5C, Table S3) and no valuable terms in up-regulated DEGs (Fig.5D, Table S3) were found comparing with SCI (solvent control) group. These down-regulated DEGs were protein binding, binding and sequence-specific DNA binding.

KEGG enrichment analysis of DEGs

We use scatter plot to express KEGG enrichment analysis of DEGs. In SCI (solvent control) vs sham, the up-regulated DEGs were most enriched in TNF, NF-kappa B, Cytokine-cytokine receptor interaction, Toll-like receptor, Leukocyte transendothelial migration, PI3K-Akt, Focal adhesion, Apoptosis, etc (Fig.6A, Table S4); the down-regulated DEGs were most enriched in Glutamatergic synapse, Basal cell carcinoma, Axon guidance, Other glycan degradation and Nicotine addiction (Fig.6B, Table S4). In SCI (probenecid) vs SCI (solvent control), only “ECM-receptor interaction” was enriched in the up-regulated DEGs (Fig.7A, Table S5); the down-regulated DEGs were enriched in Cell adhesion molecules (CAMs), Malaria, Leukocyte transendothelial migration, ECM-receptor interaction, PI3K-Akt signaling pathway, Hematopoietic cell lineage, Focal adhesion, Rap1 signaling pathway and Amoebiasis (Fig.7B, Table S5).

Discussion

Recent studies have found that probenecid has neuroprotective and repairing effects in the process of brain disorders (Wei et al. 2015; Xiong et al. 2014). However, its effect on genome-wide transcription in acute spinal cord injury (SCI) is still unknown. Therefore, in this study, RNA-Seq was used to analyze the effect of probenecid on the local expression of gene transcription 8 hours after SCI. The results showed that comparing with the sham group, there were 4617 DEGs in SCI (solvent control) group, including 2904 up-regulated and 1713 down-regulated genes. Compared with the SCI (solvent control), there were 641 different genes in SCI (probenecid) group, 286 were up-regulated and 355 were down-regulated. These are consistent with others and our previous reports (Chen et al. 2013; Shi et al. 2017). It also shows that the results of this experiment are reliable. Comparing with the SCI (solvent control), we found 641 different genes in SCI (probenecid) group, 286 were up-regulated and 355 were down-regulated. To further verify the RNA-seq results, we randomly selected 9 DEGs (Itga1, Lamb1, Cldn5, Lama2, CD34, Esam, Setdb2, Agrn and Ccnt2) for RT-qPCR. The results showed that the expression patterns of these genes detected by these two methods are similar. These demonstrated that our RNA-seq results are reliable and can be used for the next analysis. These also confirmed that probenecid can alter gene transcription after SCI.

In order to further analyze the DEGs effected by probenecid, we used GO enrichment which can reflect the distribution of DEGs on GO term enriched in cell components, molecular functions and biological processes (Huang et al. 2013). In SCI (probenecid) vs SCI (solvent control), the analysis showed that there were 3 GO terms in down-regulated DEGs (protein binding, binding and sequence-specific DNA binding) and no valuable terms in up-regulated DEGs. KEGG analysis showed that the valuable signaling pathways associated with these DEGs included CAMs, Leukocyte transendothelial migration, ECM-receptor interaction, PI3K-Akt signaling pathway, Hematopoietic cell lineage, Focal adhesion, Rap1 signaling pathway, etc..

Among these signal pathways, some have been reported to be related to SCI, such as CAMs (Brook et al. 2000; Zhang et al. 2008), ECM-receptor interaction (Zhou et al. 2017), PI3K-Akt signaling pathway (Li et al. 2019a; Li et al. 2019b; Zhang et al. 2017) and Focal adhesion (Chuang et al. 2018; Graham et al. 2016; Hao et al. 2018).

Leukocyte transendothelial migration from the blood into tissues is vital for immune surveillance and inflammation (Cook-Mills 2006).There is a large amount of leukocyte infiltration in the pathological process of SCI. The infiltration of leukocytes need bind to endothelial cell adhesion molecules and then migrate between vascular endothelial cells (Wang et al. 2011). Therefore, the inhibition of Leukocyte transendothelial migration and CAMs induced by probenecid may play a role in inhibiting inflammation by weakening the infiltration of white blood cells in the injured area.

The ECM plays an important role in tissue and organ morphogenesis (Bonnans et al. 2014; Rabelink et al. 2017) and control of cellular activities such as adhesion, migration, differentiation, proliferation and apoptosis (Yue 2014). Focal adhesions are specialized intracellular sites in which aggregated integrin receptors interact with extracellular matrices, while extracellular matrices interact with intracellular actin cytoskeleton (Burridge 2017; LaFlamme et al. 2018). At the same time, focal adhesions are the result of cell-extracellular matrix (ECM) interactions (Burridge 2017; De Pascalis & Etienne-Manneville 2017). ECM and Focal adhesions are down-regulated after probenecid treatment, indicating that probenecid might improve SCI by inhibiting adhesion, migration, differentiation, proliferation and apoptosis.

It has been reported that PI3K-Akt signaling fuses a variety of extracellular and intracellular signal transduction pathways that regulate macrophage biology, including the production of pro-inflammatory cytokines, phagocytosis, autophagy and homeostasis (Vergadi et al. 2017). PI3K-Akt signal pathway is down-regulated in SCI after probenecid treatment, indicating that probenecid might improve SCI by regulating macrophages and inhibiting inflammatory pathways.

The relationship between hematopoietic cell lineage pathway and SCI was found in a report on the bioinformatics analysis of SCI (Zhu et al. 2017). Its specific role has not been reported yet, and it deserves further discussion.

Rap1 signal pathway plays an important role in regulating cell-cell and cell-matrix interactions by regulating the function of adhesion molecules (Kim et al. 2011; Pollan et al. 2018). In our study, Rap1 signaling pathway was enriched in down-regulated DEGs of SCI after probenecid treatment, suggesting that probenecid may inhibit cell adhesion and polarization by inhibiting the Rap1 signaling pathway, thereby inhibiting inflammation.

Conclusions

Acute SCI can lead to changes of mRNAs in injured spinal cords. These mRNAs and their related pathways could provide some explanations for the pathological mechanism of acute SCI.

More interestingly, we also demonstrate that probenecid can lead to gene expression inhibitions in the acute injured spinal cord. These down-regulated DEGs and their associated signaling pathways, such as Focal adhesion, Leukocyte transendothelial migration, ECM-receptor interaction, PI3K-Akt, Rap1, are mainly related to inflammatory response, local hypoxia, macrophage differentiation, adhesion migration and apoptosis of local cells. This suggests that the application of probenecid in acute phase can improve the local microenvironment of SCI. However, whether probenecid can be used as a therapeutic drug for SCI still needs to be further explored. Next, the detailed research on this subject will be conducted by combining animal models and clinical practice.

Declaration of Conflicting Interests

The authors declare that they have no competing interests.

Funding

This study was supported by grants from the National Natural Science Foundation of China (Nos. 81571194, 81772321).

References

Ahuja CS, Nori S, Tetreault L, Wilson J, Kwon B, Harrop J, Choi D, and Fehlings MG. 2017. Traumatic Spinal Cord Injury-Repair and Regeneration. *Neurosurgery* 80:S9-S22. 10.1093/neuros/nyw080

Baranova A, Ivanov D, Petrash N, Pestova A, Skoblov M, Kelmanson I, Shagin D, Nazarenko S, Geraymovych E, Litvin O, Tiunova A, Born TL, Usman N, Staroverov D, Lukyanov S, and Panchin Y. 2004. The mammalian pannexin family is homologous to the invertebrate innexin gap junction proteins. *Genomics* 83:706-716. 10.1016/j.ygeno.2003.09.025

Bonnans C, Chou J, and Werb Z. 2014. Remodelling the extracellular matrix in development and disease. *Nat Rev Mol Cell Biol* 15:786-801. 10.1038/nrm3904

Brook GA, Houweling DA, Gieling RG, Hermanns T, Joosten EA, Bar DP, Gispen WH, Schmitt AB, Leprince P, Noth J, and Nacimiento W. 2000. Attempted endogenous tissue repair following experimental spinal cord injury in the rat: involvement of cell adhesion molecules L1 and NCAM? *Eur J Neurosci* 12:3224-3238.

Burridge K. 2017. Focal adhesions: a personal perspective on a half century of progress. *FEBS J* 284:3355-3361. 10.1111/febs.14195

Chen K, Deng S, Lu H, Zheng Y, Yang G, Kim D, Cao Q, and Wu JQ. 2013. RNA-seq characterization of spinal cord injury transcriptome in acute/subacute phases: a resource for understanding the pathology at the systems level. *PLoS One* 8:e72567. 10.1371/journal.pone.0072567

Chuang YC, Lee CH, Sun WH, and Chen CC. 2018. Involvement of advillin in somatosensory neuron subtype-specific axon regeneration and neuropathic pain. *Proc Natl Acad Sci U S A* 115:E8557-E8566. 10.1073/pnas.1716470115

Cook-Mills JM. 2006. Hydrogen peroxide activation of endothelial cell-associated MMPs during VCAM-1-dependent leukocyte migration. *Cell Mol Biol (Noisy-le-grand)* 52:8-16.

De Pascalis C, and Etienne-Manneville S. 2017. Single and collective cell migration: the mechanics of adhesions. *Mol Biol Cell* 28:1833-1846. 10.1091/mbc.E17-03-0134

Friedli L, Rosenzweig ES, Barraud Q, Schubert M, Dominici N, Awai L, Nielson JL, Musienko P, Nout-Lomas Y, Zhong H, Zdunowski S, Roy RR, Strand SC, van den Brand R, Havton LA, Beattie MS, Bresnahan JC, Bezard E, Bloch J, Edgerton VR, Ferguson AR, Curt A, Tuszynski MH, and Courtine G. 2015. Pronounced species divergence in corticospinal tract reorganization and functional recovery after lateralized spinal cord injury favors primates. *Sci Transl Med* 7:302ra134. 10.1126/scitranslmed.aac5811

Geisler FH, Coleman WP, Benzel E, Ducker T, and Hurlbert RJ. 2002. Spinal cord injury. *Lancet* 360:1883; author reply 1884. 10.1016/s0140-6736(02)11744-2

Graham ZA, Qin W, Harlow LC, Ross NH, Bauman WA, Gallagher PM, and Cardozo CP. 2016. Focal adhesion kinase signaling is decreased 56 days following spinal cord injury in rat gastrocnemius. *Spinal Cord* 54:502-509. 10.1038/sc.2015.183

Hagos FT, Daood MJ, Ocque JA, Nolin TD, Bayir H, Poloyac SM, Kochanek PM, Clark RS, and Empey PE. 2017. Probenecid, an organic anion transporter 1 and 3 inhibitor, increases plasma and brain exposure of N-acetylcysteine. *Xenobiotica* 47:346-353. 10.1080/00498254.2016.1187777

Hainz N, Wolf S, Beck A, Wagenpfeil S, Tschernig T, and Meier C. 2017. Probenecid arrests the progression of pronounced clinical symptoms in a mouse model of multiple sclerosis. *Sci Rep* 7:17214. 10.1038/s41598-017-17517-5

Hao M, Ji XR, Chen H, Zhang W, Zhang LC, Zhang LH, Tang PF, and Lu N. 2018. Cell cycle and complement inhibitors may be specific for treatment of spinal cord injury in aged and young mice: Transcriptomic analyses. *Neural Regen Res* 13:518-527. 10.4103/1673-5374.226405

Huang Q, Wu LY, Wang Y, and Zhang XS. 2013. GOMA: functional enrichment analysis tool based on GO modules. *Chin J Cancer* 32:195-204. 10.5732/cjc.012.10151

Kim C, Ye F, and Ginsberg MH. 2011. Regulation of integrin activation. *Annu Rev Cell Dev Biol* 27:321-345. 10.1146/annurev-cellbio-100109-104104

Krueger H, Noonan VK, Trenaman LM, Joshi P, and Rivers CS. 2013. The economic burden of traumatic spinal cord injury in Canada. *Chronic Dis Inj Can* 33:113-122.

LaFlamme SE, Mathew-Steiner S, Singh N, Colello-Borges D, and Nieves B. 2018. Integrin and microtubule crosstalk in the regulation of cellular processes. *Cell Mol Life Sci* 75:4177-4185. 10.1007/s00018-018-2913-x

Li H, Zhang X, Qi X, Zhu X, and Cheng L. 2019a. Icariin Inhibits Endoplasmic Reticulum Stress-induced Neuronal Apoptosis after Spinal Cord Injury through Modulating the PI3K/AKT Signaling Pathway. *Int J Biol Sci* 15:277-286. 10.7150/ijbs.30348

Li Y, Guo Y, Fan Y, Tian H, Li K, and Mei X. 2019b. Melatonin Enhances Autophagy and Reduces Apoptosis to Promote Locomotor Recovery in Spinal Cord Injury via the PI3K/AKT/mTOR Signaling Pathway. *Neurochem Res* 44:2007-2019. 10.1007/s11064-019-02838-w

Livak KJ, and Schmittgen TD. 2001. Analysis of relative gene expression data using real-time quantitative PCR and the 2(-Delta Delta C(T)) Method. *Methods* 25:402-408. 10.1006/meth.2001.1262

Mawhinney LJ, de Rivero Vaccari JP, Dale GA, Keane RW, and Bramlett HM. 2011. Heightened inflammasome activation is linked to age-related cognitive impairment in Fischer 344 rats. *BMC Neurosci* 12:123. 10.1186/1471-2202-12-123

McDonald JW, and Sadowsky C. 2002. Spinal-cord injury. *Lancet* 359:417-425. 10.1016/S0140-6736(02)07603-1

Oyinbo CA. 2011. Secondary injury mechanisms in traumatic spinal cord injury: a nugget of this multiply cascade. *Acta Neurobiol Exp (Wars)* 71:281-299.

Papadopoulos MC, and Verkman AS. 2008. Potential utility of aquaporin modulators for therapy of brain disorders. *Prog Brain Res* 170:589-601. 10.1016/S0079-6123(08)00446-9

Pollan SG, Huang F, Sperger JM, Lang JM, Morrissey C, Cress AE, Chu CY, Bhowmick NA, You S, Freeman MR, Spassov DS, Moasser MM, Carter WG, Satapathy SR, Shah K, and Knudsen BS. 2018. Regulation of inside-out beta1-integrin activation by CDCP1. *Oncogene* 37:2817-2836. 10.1038/s41388-018-0142-2

Qiu J. 2009. China Spinal Cord Injury Network: changes from within. *Lancet Neurol* 8:606-607. 10.1016/S1474-4422(09)70162-0

Rabelink TJ, van den Berg BM, Garsen M, Wang G, Elkin M, and van der Vlag J. 2017. Heparanase: roles in cell survival, extracellular matrix remodelling and the development of kidney disease. *Nat Rev Nephrol* 13:201-212. 10.1038/nrneph.2017.6

Shi LL, Zhang N, Xie XM, Chen YJ, Wang R, Shen L, Zhou JS, Hu JG, and Lu HZ. 2017. Transcriptome profile of rat genes in injured spinal cord at different stages by RNA-sequencing. *BMC Genomics* 18:173. 10.1186/s12864-017-3532-x

Singh A, Tetreault L, Kalsi-Ryan S, Nouri A, and Fehlings MG. 2014. Global prevalence and incidence of traumatic spinal cord injury. *Clin Epidemiol* 6:309-331. 10.2147/CLEP.S68889

Tollner K, Brandt C, Romermann K, and Loscher W. 2015. The organic anion transport inhibitor probenecid increases brain concentrations of the NKCC1 inhibitor bumetanide. *Eur J Pharmacol* 746:167-173. 10.1016/j.ejphar.2014.11.019

Tran AP, Warren PM, and Silver J. 2018. The Biology of Regeneration Failure and Success After Spinal Cord Injury. *Physiol Rev* 98:881-917. 10.1152/physrev.00017.2017

Vergadi E, Ieronymaki E, Lyroni K, Vaporidi K, and Tsatsanis C. 2017. Akt Signaling Pathway in Macrophage Activation and M1/M2 Polarization. *J Immunol* 198:1006-1014. 10.4049/jimmunol.1601515

Wang JG, Williams JC, Davis BK, Jacobson K, Doerschuk CM, Ting JP, and Mackman N. 2011. Monocytic microparticles activate endothelial cells in an IL-1beta-dependent manner. *Blood* 118:2366-2374. 10.1182/blood-2011-01-330878

Wei R, Wang J, Xu Y, Yin B, He F, Du Y, Peng G, and Luo B. 2015. Probenecid protects against cerebral ischemia/reperfusion injury by inhibiting lysosomal and inflammatory damage in rats. *Neuroscience* 301:168-177. 10.1016/j.neuroscience.2015.05.070

Xiong XX, Gu LJ, Shen J, Kang XH, Zheng YY, Yue SB, and Zhu SM. 2014. Probenecid protects against transient focal cerebral ischemic injury by inhibiting HMGB1 release and attenuating AQP4 expression in mice. *Neurochem Res* 39:216-224. 10.1007/s11064-013-1212-z

Yue B. 2014. Biology of the extracellular matrix: an overview. *J Glaucoma* 23:S20-23. 10.1097/IJG.0000000000000108

Zhang F, Ru N, Shang ZH, Chen JF, Yan C, Li Y, and Liang J. 2017. Daidzein ameliorates spinal cord ischemia/reperfusion injury-induced neurological function deficits in Sprague-Dawley rats through PI3K/Akt signaling pathway. *Exp Ther Med* 14:4878-4886. 10.3892/etm.2017.5166

Zhang Y, Yeh J, Richardson PM, and Bo X. 2008. Cell adhesion molecules of the immunoglobulin superfamily in axonal regeneration and neural repair. *Restor Neurol Neurosci* 26:81-96.

Zhou J, Xiong Q, Chen H, Yang C, and Fan Y. 2017. Identification of the Spinal Expression Profile of Non-coding RNAs Involved in Neuropathic Pain Following Spared Nerve Injury by Sequence Analysis. *Front Mol Neurosci* 10:91. 10.3389/fnmol.2017.00091

Zhu Z, Wang D, Jiao W, Chen G, Cao Y, Zhang Q, and Wang J. 2017. Bioinformatics analyses of pathways and gene predictions in IL-1alpha and IL-1beta knockout mice with spinal cord injury. *Acta Histochem* 119:663-670. 10.1016/j.acthis.2017.07.007

Figures

Figure 1 PCA analysis

PCA analysis was performed using three principal components (PC1, 2, and 3) to demonstrate the source of variance (n=3).

Figure 2 Volcano map of DEGs

Red, green and blue dots represent significantly up-regulated, down-regulated and no changed gene expressions, respectively. (A) SCI (solvent control) vs Sham; (B) SCI (probenecid) vs SCI (solvent control).

Figure 3 RT-qPCR verification of DEGs characterized by RNA-Seq

The longitudinal coordinates in RNA-Seq were the mRNA expression level (read counts). The longitudinal coordinates in RT-qPCR were the mRNA expression level calculated by using the $^{\Delta\Delta}$Ct method and expressed relative to the value in the sham group (designated as 1). All data were calculated with mean ± standard deviation (n = 6).

Figure 4 Hierarchical cluster analysis of DEGs

From red to blue, the gene expression is from up to down. sham: sham group; SCI_C: SCI (solvent control) group; SCI_P: SCI (probenecid) group.

Figure 5 GO enrichment analysis of DEGs

We list the 30 richest Go terms. The asterisk (*) represent significant enrichment terms ($P \leq 0.05$). A: GO analysis of up-regulated DEGs in SCI (solvent control) vs sham group; B: GO analysis of down-regulated DEGs in SCI (solvent control) vs sham group; C: GO analysis of down-regulated DEGs in SCI (probenecid) vs SCI (solvent control) group; D: GO analysis of up-regulated DEGs in SCI (probenecid) vs SCI (solvent control) group (D).

Figure 6 KEGG enrichment analyses of DEGs in SCI (solvent control) vs sham group

The 20 most enriched KEGG pathways were shown. A: KEGG pathways in up-regulated DEGs; B: KEGG pathways in down-regulated DEGs.

Figure 7 KEGG enrichment analyses of DEGs in SCI (probenecid) vs SCI (solvent control)

The 20 most enriched KEGG pathways were shown. A: KEGG pathways in up-regulated DEGs; B: KEGG pathways in down-regulated DEGs.

Tables

Table 1 PCR primers used in the study
Table 2 Summary of sequence assembly after Illumina sequencing

Supplementary materials

Table S1 The DEGs of different groups
Table S2 GO enrichment analysis of SCI (solvent control) vs sham group
Table S3 GO enrichment analysis of SCI (probenecid) vs SCI (solvent control) group
Table S4 KEGG analysis of SCI (solvent control) vs sham group
Table S5 KEGG analysis of SCI (probenecid) vs SCI (solvent control) group

Figure 1

Figure 1 PCA analysis

PCA analysis was performed using three principal components (PC1, 2, and 3) to demonstrate the source of variance (n=3).

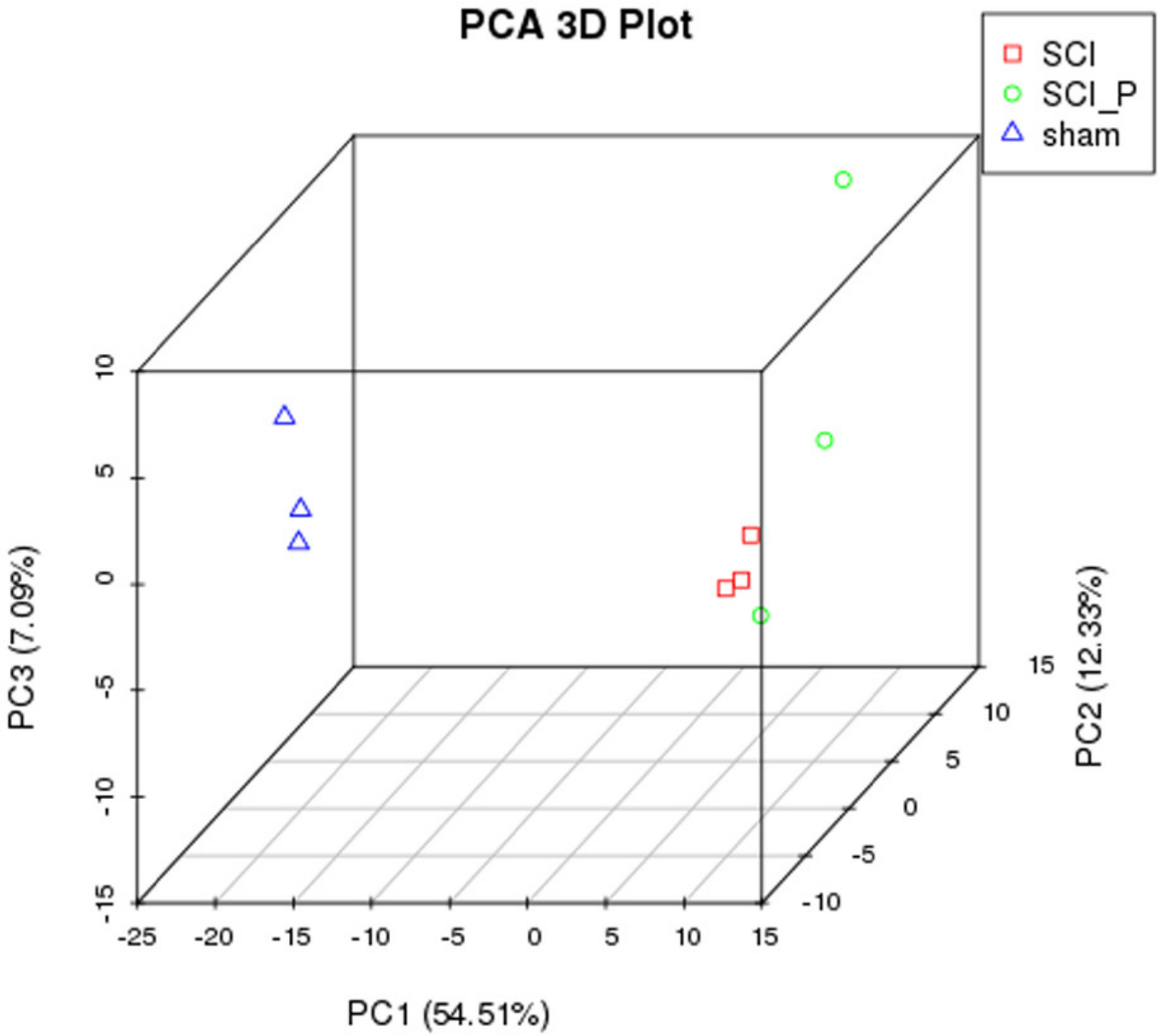

Figure 2

Figure 2 Volcano map of DEGs

Red, green and blue dots represent significantly up-regulated, down-regulated and no changed gene expressions, respectively. (A) SCI (solvent control) vs Sham; (B) SCI (probenecid) vs SCI (solvent control).

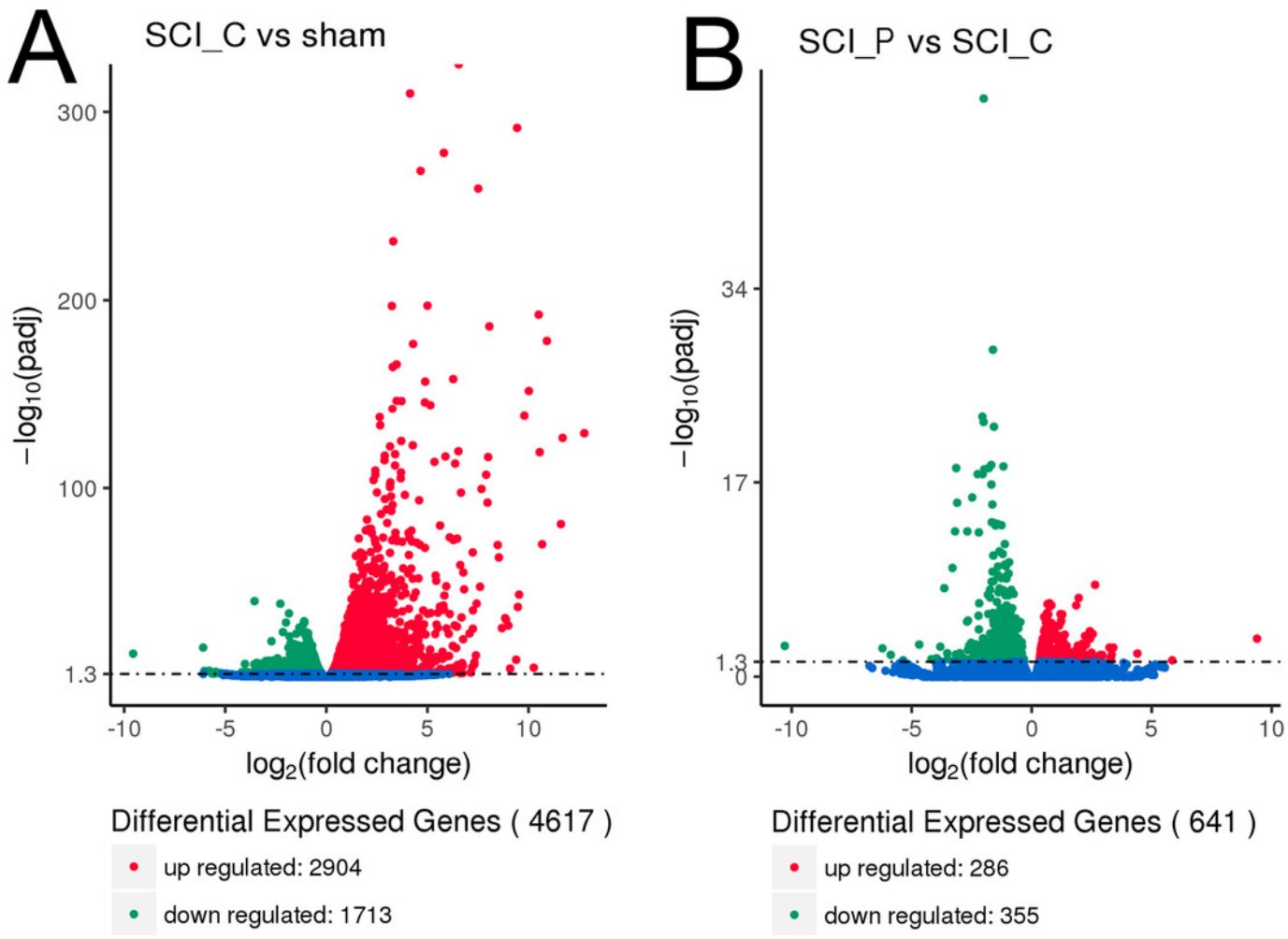

Figure 3

Figure 3 RT-qPCR verification of DEGs characterized by RNA-Seq

The longitudinal coordinates in RNA-Seq were the mRNA expression level (read counts), which can be used directly to compare the difference in gene expression between the samples. The longitudinal coordinates in RT-qPCR were the mRNA expression level calculated by using the $^{\Delta\Delta}$Ct method and expressed relative to the value in the sham group (designated as 1). All data were calculated with mean ± standard deviation (n = 6).

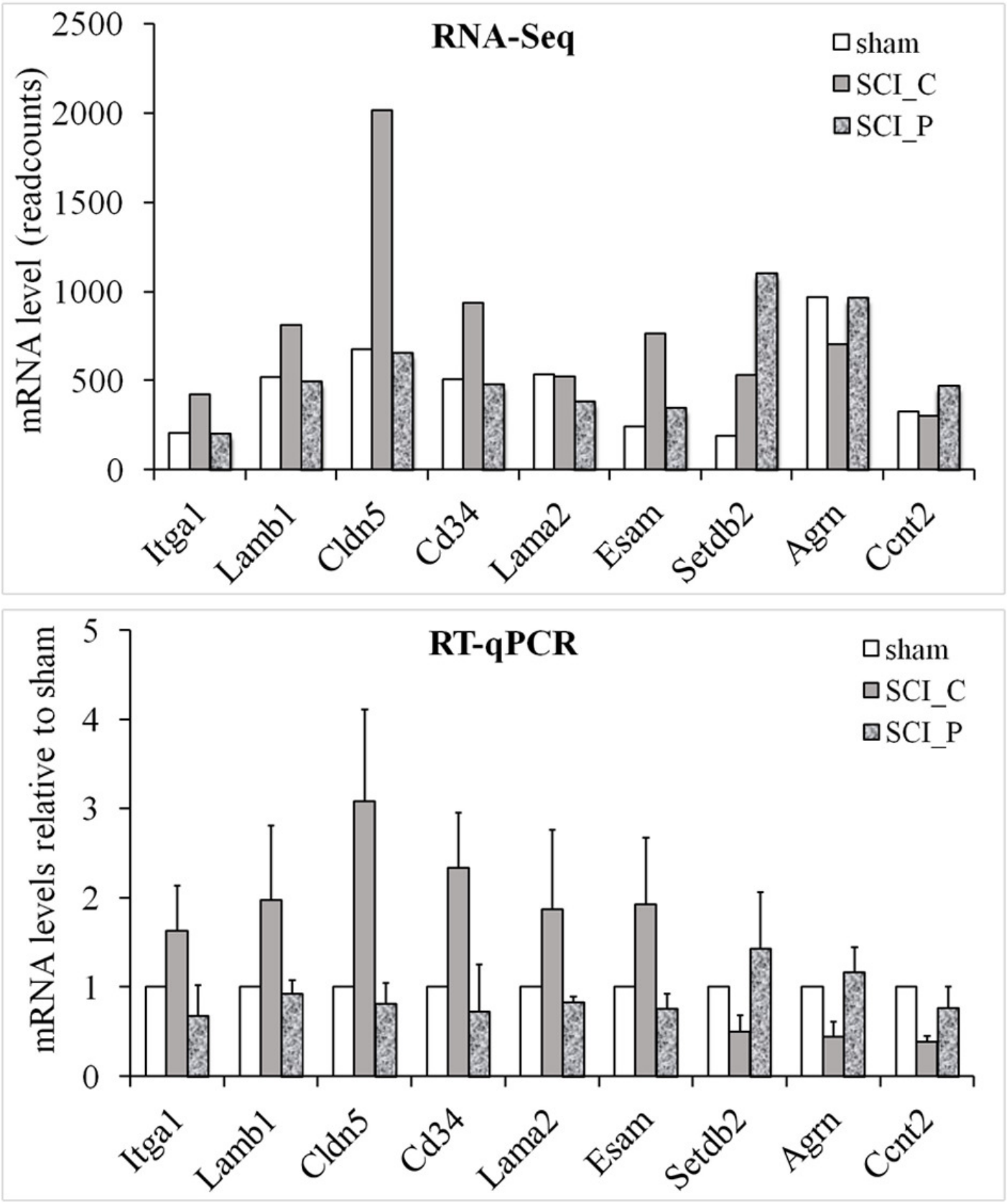
RNA-Seq
mRNA level (readcounts)
2500
2000
1500
1000
500
0
sham
SCI_C
SCI_P
Itga1
Lamb1
Cldn5
Cd34
Lama2
Esam
Setdb2
Agrn
Ccnt2
RT-qPCR
mRNA levels relative to sham
5
4
3
2
1
0
sham
SCI_C
SCI_P
Itga1
Lamb1
Cldn5
Cd34
Lama2
Esam
Setdb2
Agrn
Ccnt2

Figure 4

Figure 4 Hierarchical cluster analysis of DEGs

Based on the similarity of gene expression patterns, the DEGs were divided into multiple expression clusters. From red to blue, the gene expression is from up to down. sham: sham group; SCI_C: SCI (solvent control) group; SCI_P:SCI (probenecid) group.

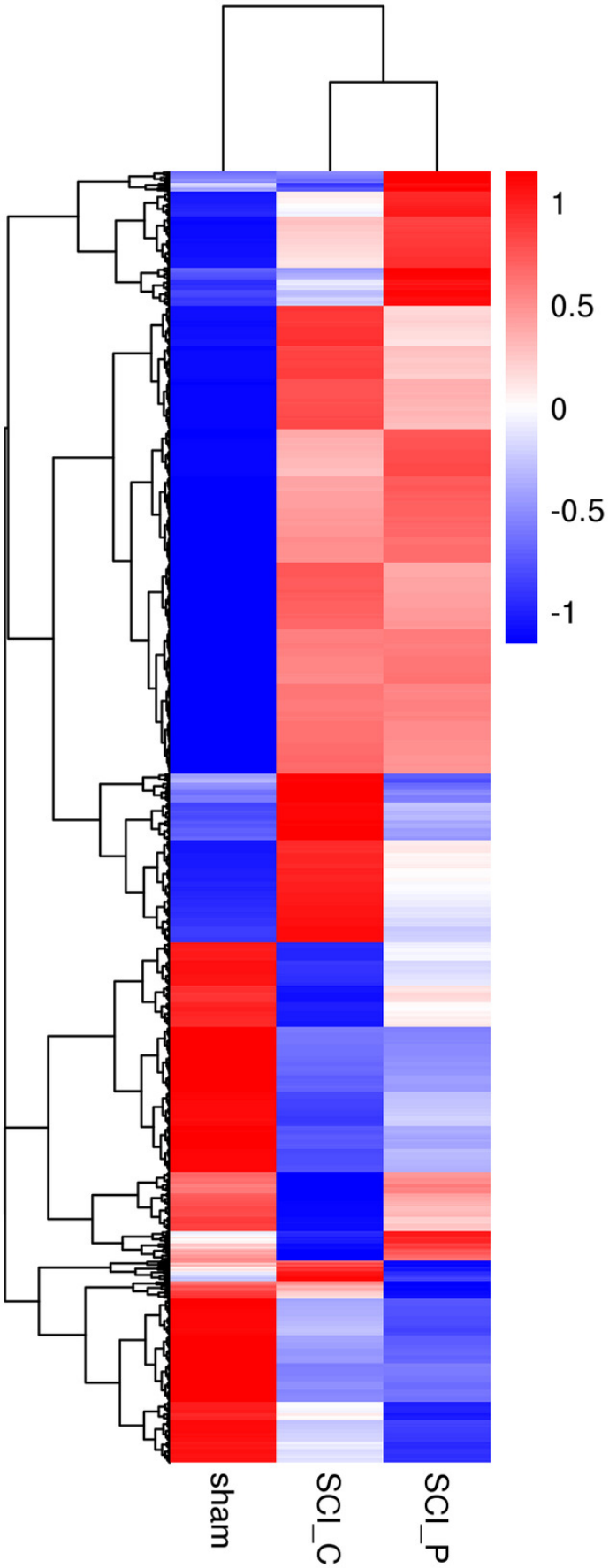
1
0.5
0
-0.5
-1
sham
SCI_C
SCI_P

Figure 5

Figure 5 GO enrichment analysis of DEGs

We list the 30 richest Go terms. The asterisk (*) represent significant enrichment terms ($P \leq 0.05$). A: GO analysis of up-regulated DEGs in SCI (solvent control) vs sham group; B: GO analysis of down-regulated DEGs in SCI (solvent control) vs sham group; C: GO analysis of down-regulated DEGs in SCI (probenecid) vs SCI (solvent control) group; D: GO analysis of up-regulated DEGs in SCI (probenecid) vs SCI (solvent control) group (D).

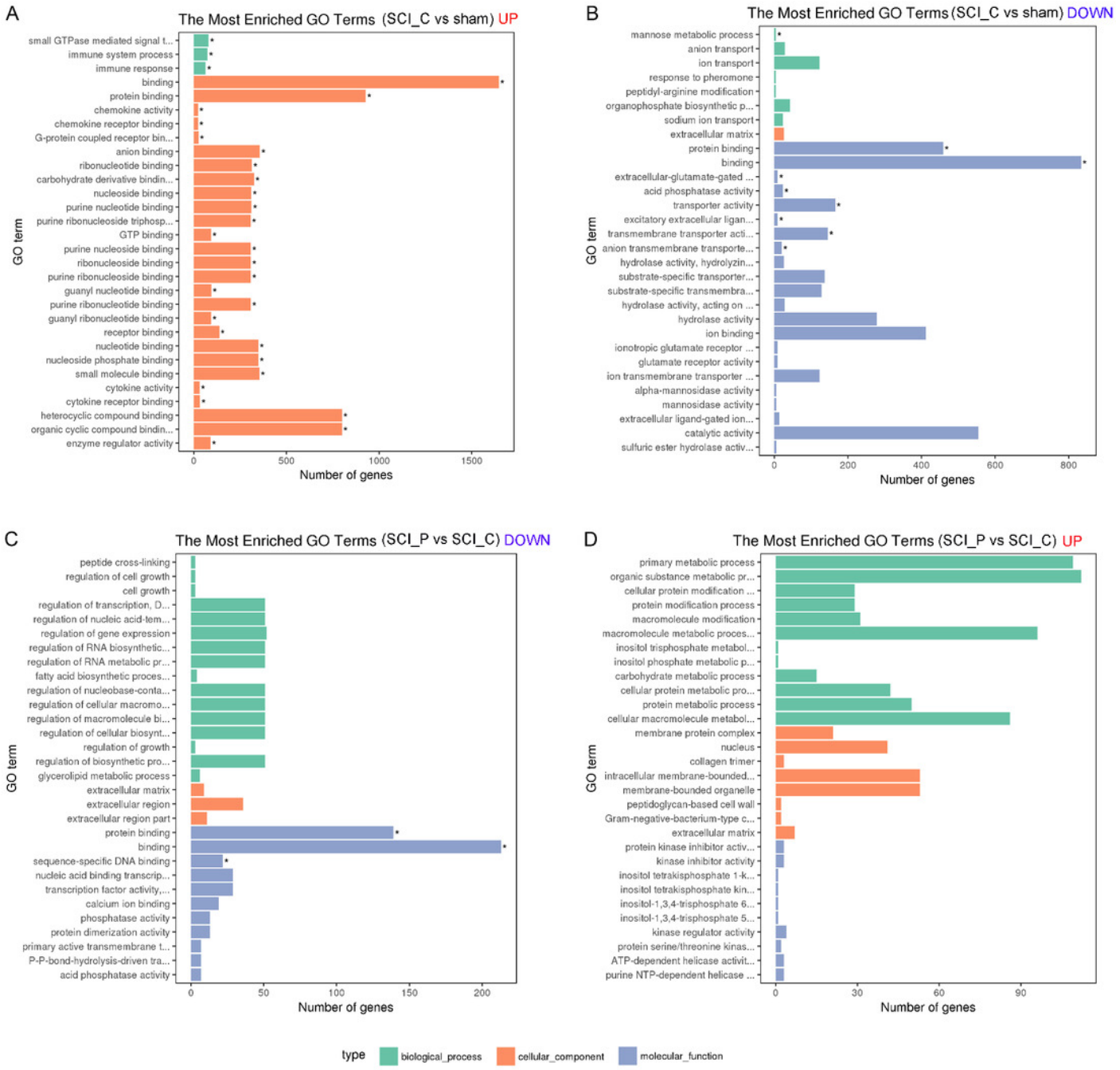
A
The Most Enriched GO Terms (SCI_C vs sham) UP
small GTPase mediated signal t...
immune system process
immune response
binding
protein binding
chemokine activity
chemokine receptor binding
G-protein coupled receptor bin...
anion binding
ribonucleotide binding
carbohydrate derivative bindin...
nucleoside binding
purine nucleotide binding
purine ribonucleoside triphosp...
GTP binding
purine nucleoside binding
ribonucleoside binding
purine ribonucleoside binding
guanyl nucleotide binding
purine ribonucleotide binding
guanyl ribonucleotide binding
receptor binding
nucleotide binding
nucleoside phosphate binding
small molecule binding
cytokine activity
cytokine receptor binding
heterocyclic compound binding
organic cyclic compound bindin...
enzyme regulator activity
GO term
0
500
1000
1500
Number of genes
B
The Most Enriched GO Terms (SCI_C vs sham) DOWN
mannose metabolic process
anion transport
ion transport
response to pheromone
peptidyl-arginine modification
organophosphate biosynthetic p...
sodium ion transport
extracellular matrix
protein binding
binding
extracellular-glutamate-gated ...
acid phosphatase activity
transporter activity
excitatory extracellular ligan...
transmembrane transporter acti...
anion transmembrane transporte...
hydrolase activity, hydrolyzin...
substrate-specific transporter...
substrate-specific transmembra...
hydrolase activity, acting on ...
hydrolase activity
ion binding
ionotropic glutamate receptor ...
glutamate receptor activity
ion transmembrane transporter ...
alpha-mannosidase activity
mannosidase activity
extracellular ligand-gated ion...
catalytic activity
sulfuric ester hydrolase activ...
GO term
0
200
400
600
800
Number of genes
C
The Most Enriched GO Terms (SCI_P vs SCI_C) DOWN
peptide cross-linking
regulation of cell growth
cell growth
regulation of transcription, D...
regulation of nucleic acid-tem...
regulation of gene expression
regulation of RNA biosynthetic...
regulation of RNA metabolic pr...
fatty acid biosynthetic proces...
regulation of nucleobase-conta...
regulation of cellular macromo...
regulation of macromolecule bi...
regulation of cellular biosynt...
regulation of growth
regulation of biosynthetic pro...
glycerolipid metabolic process
extracellular matrix
extracellular region
extracellular region part
protein binding
binding
sequence-specific DNA binding
nucleic acid binding transcrip...
transcription factor activity,...
calcium ion binding
phosphatase activity
protein dimerization activity
primary active transmembrane t...
P-P-bond-hydrolysis-driven tra...
acid phosphatase activity
GO term
0
50
100
150
200
Number of genes
D
The Most Enriched GO Terms (SCI_P vs SCI_C) UP
primary metabolic process
organic substance metabolic pr...
cellular protein modification ...
protein modification process
macromolecule modification
macromolecule metabolic proces...
inositol trisphosphate metabol...
inositol phosphate metabolic p...
carbohydrate metabolic process
cellular protein metabolic pro...
protein metabolic process
cellular macromolecule metabol...
membrane protein complex
nucleus
collagen trimer
intracellular membrane-bounded...
membrane-bounded organelle
peptidoglycan-based cell wall
Gram-negative-bacterium-type c...
extracellular matrix
protein kinase inhibitor activ...
kinase inhibitor activity
inositol tetrakisphosphate 1-k...
inositol tetrakisphosphate kin...
inositol-1,3,4-trisphosphate 6...
inositol-1,3,4-trisphosphate 5...
kinase regulator activity
protein serine/threonine kinas...
ATP-dependent helicase activit...
purine NTP-dependent helicase ...
GO term
0
30
60
90
Number of genes
type
biological_process
cellular_component
molecular_function

Figure 6

Figure 6 KEGG enrichment analyses of DEGs in SCI (solvent control) vs sham group

The 20 most enriched KEGG pathways were shown. A: KEGG pathways in up-regulated DEGs; B: KEGG pathways in down-regulated DEGs.

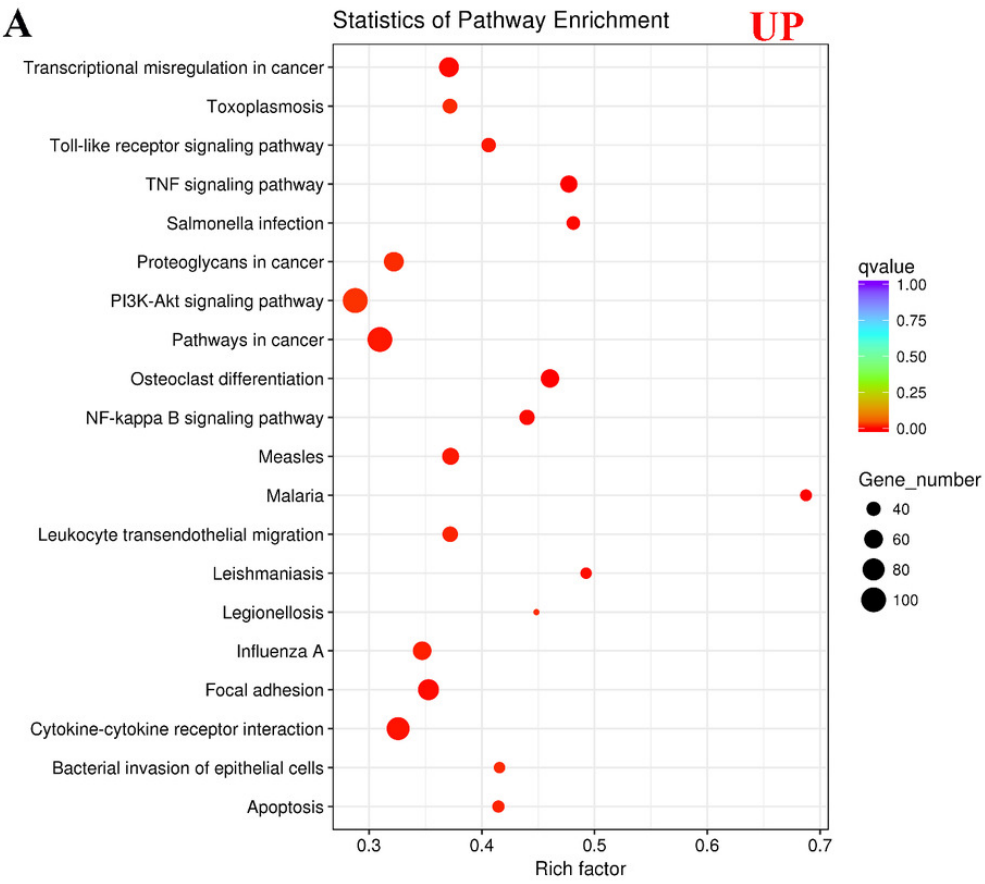
A
Statistics of Pathway Enrichment
UP
Transcriptional misregulation in cancer
Toxoplasmosis
Toll-like receptor signaling pathway
TNF signaling pathway
Salmonella infection
Proteoglycans in cancer
PI3K-Akt signaling pathway
Pathways in cancer
Osteoclast differentiation
NF-kappa B signaling pathway
Measles
Malaria
Leukocyte transendothelial migration
Leishmaniasis
Legionellosis
Influenza A
Focal adhesion
Cytokine-cytokine receptor interaction
Bacterial invasion of epithelial cells
Apoptosis
0.3
0.4
0.5
0.6
0.7
Rich factor
qvalue
1.00
0.75
0.50
0.25
0.00
Gene_number
40
60
80
100

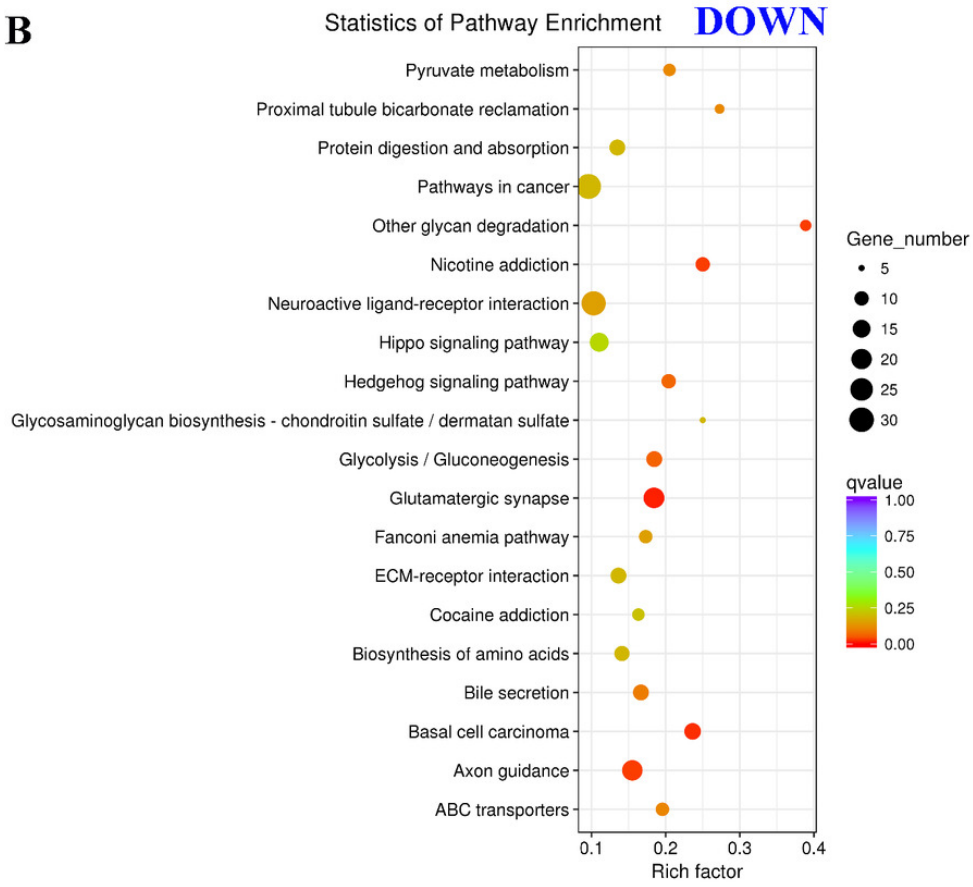
B
Statistics of Pathway Enrichment
DOWN
Pyruvate metabolism
Proximal tubule bicarbonate reclamation
Protein digestion and absorption
Pathways in cancer
Other glycan degradation
Nicotine addiction
Neuroactive ligand-receptor interaction
Hippo signaling pathway
Hedgehog signaling pathway
Glycosaminoglycan biosynthesis - chondroitin sulfate / dermatan sulfate
Glycolysis / Gluconeogenesis
Glutamatergic synapse
Fanconi anemia pathway
ECM-receptor interaction
Cocaine addiction
Biosynthesis of amino acids
Bile secretion
Basal cell carcinoma
Axon guidance
ABC transporters
0.1
0.2
0.3
0.4
Rich factor
Gene_number
5
10
15
20
25
30
qvalue
1.00
0.75
0.50
0.25
0.00

Figure 7

Figure 7 KEGG enrichment analyses of DEGs in SCI (probenecid) vs SCI (solvent control)

The 20 most enriched KEGG pathways were shown. A: KEGG pathways in up-regulated DEGs; B: KEGG pathways in down-regulated DEGs.


A
Statistics of Pathway Enrichment
UP
Vitamin B6 metabolism
Viral myocarditis
Ubiquitin mediated proteolysis
Spliceosome
RNA degradation
Protein digestion and absorption
Primary bile acid biosynthesis
Platelet activation
PI3K-Akt signaling pathway
Pantothenate and CoA biosynthesis
Other glycan degradation
Lysine degradation
Legionellosis
Focal adhesion
Fanconi anemia pathway
Epstein-Barr virus infection
ECM-receptor interaction
Circadian entrainment
Axon guidance
Amoebiasis
0.03
0.06
0.09
Rich factor
Gene_number
1
2
3
4
5
6
7
qvalue
1.00
0.75
0.50
0.25
0.00

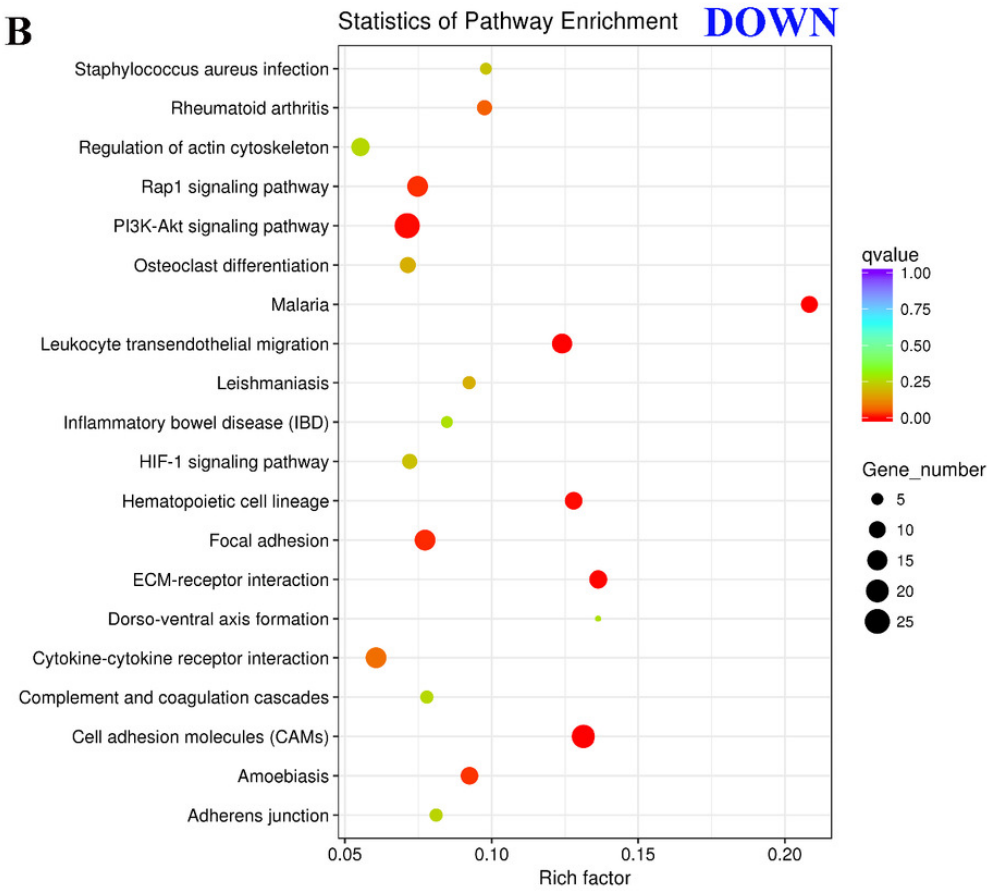
B
Statistics of Pathway Enrichment
DOWN
Staphylococcus aureus infection
Rheumatoid arthritis
Regulation of actin cytoskeleton
Rap1 signaling pathway
PI3K-Akt signaling pathway
Osteoclast differentiation
Malaria
Leukocyte transendothelial migration
Leishmaniasis
Inflammatory bowel disease (IBD)
HIF-1 signaling pathway
Hematopoietic cell lineage
Focal adhesion
ECM-receptor interaction
Dorso-ventral axis formation
Cytokine-cytokine receptor interaction
Complement and coagulation cascades
Cell adhesion molecules (CAMs)
Amoebiasis
Adherens junction
0.05
0.10
0.15
0.20
Rich factor
qvalue
1.00
0.75
0.50
0.25
0.00
Gene_number
5
10
15
20
25

Table 1(on next page)

Table 1 PCR primers used in the study

No

1 **Table 1 Real-time PCR primers used in the study**

2

Gene	Forward primer 5' - 3'	Reverse primer 5' - 3'
Itga1	AGACTCTGGGACTTACCGCT	CCTCGTCTGATTCACAGCGT
lamb1	TGCCTTTTCTCCCCGCTACC	CCATGTCCAGTCCTCGCAGA
Cldn5	TTCTATGATCCGACGGTGCC	CTTGACCGGGAAGCTGAACT
CD34	ACCACAGACTTCCCCAACTG	CATATGGCTCGGTGGGTGAT
lama2	GCATTAGTGAGCCGCCCTAT	TCTTTCAGGTCTCGTGTGGC
Esam	AGACTCTGGGACTTACCGCT	GGTCACATTGGTCCCGACAT
Setdb2	CCACAAATGGAGATCATACACCT	GCAGTGGGGCTTCCTTTTTC
Agrn	CTCTGCCACTGGAACACAGA	GGAAAAGCAGCACCGCAAAG
Ccnt2	AGCAAGGATTTGGCACAGAC	CTCTAGGGTAACCGTGGGGT
beta-actin	AGAAGCTGTGCTATGTTGCTCTA	ACCCAAGAAGGAAGGCTGGAAAA

Table 2(on next page)

Table 2 Summary of sequence assembly after Illumina sequencing

Sham: Sham_1, Sham_2, Sham_3; SCI (solvent control): SCI_C1, SCI_C2, SCI_C3; SCI (probenecid): SCI_P1, SCI_P2, SCI_P3; Q20: The percentage of bases with a Phred value > 20; Q30: The percentage of bases with a Phred value > 30.

Table 2 Summary of sequence assembly after Illumina sequencing

Sample name	Raw reads	Clean reads	clean bases	Error rate (%)	Q20 (%)	Q30 (%)	GC content (%)
Sham_1	56509230	55796658	8.37G	0.03	97.73	93.95	51.23
Sham_2	48848744	48226002	7.23G	0.03	97.6	93.67	51.71
Sham_3	58228350	57459748	8.62G	0.03	97.67	93.78	51.42
SCI_C1	58862872	58126844	8.72G	0.03	97.88	94.31	51.39
SCI_C2	56980070	56166058	8.42G	0.03	97.74	94.03	51.42
SCI_C3	59804518	58798224	8.82G	0.03	97.63	93.74	51.02
SCI_P1	54853344	53996254	8.1G	0.03	97.72	93.91	50.93
SCI_P2	56322736	55540308	8.33G	0.03	97.87	94.27	50.94
SCI_P3	61037096	60037772	9.01G	0.03	97.71	93.89	50.92

Sham: Sham_1, Sham_2, Sham_3; SCI (solvent control): SCI_C1, SCI_C2, SCI_C3; SCI (probenecid): SCI_P1, SCI_P2, SCI_P3;

Q20: The percentage of bases with a Phred value > 20;

Q30: The percentage of bases with a Phred value > 30.